Whole-body Vibration Attenuates Pyroptosis-Mediated Inflammation but Accelerates Progression of Intervertebral Disc Degeneration

Fang-da Fu
Institute of Orthopaedics and Traumatology
Sai Yao
Institute of Orthopaedics and Traumatology
Zhi-tao Sun
Department of orthopaedics
Cheng-cong Zhou
Institute of Orthopaedics and Traumatology
Huan Yu
Institute of Orthopaedics and Traumatology
Huan Luo
Department of Pharmacy
Zhiyong Pan
first clinical college of zhejiang chinese medical university
Hong-ting Jin
Institute of Orthopaedics and Traumatology
Pei-jian Tong
Institute of Orthopaedics and Traumatology
Di Chen
Department of Orthopaedics
Cheng-liang Wu
Institute of Orthopaedics and Traumatology
Hongfeng RUAN (rhf@zcmu.edu.cn)
Institute of orthopaedics and traumatology https://orcid.org/0000-0001-8868-9313

Research article

Keywords: Whole-body vibration, Intervertebral disc degeneration, Sensory nerve invasion, Pyroptosis, Wnt signaling pathway

Posted Date: March 20th, 2020

DOI: https://doi.org/10.21203/rs.3.rs-18129/v1

Abstract

Background

Whole body vibration (WBV) is a non-pharmaceutical therapy that has been widely incorporated into clinical practice for musculoskeletal disorders, including low back pain (LBP). Intervertebral disc (IVD) degeneration (IVDD) is clinically associated with LBP and is known as the main cause for LBP. However, cumulative evidence also suggested WBV might have an adverse impact on IVDs. Moreover, previous studies have been focusing on the effects of WBV on healthy mice, rather than those suffering from IVDD. Thus, uncertainties still exist concerning the effects of WBV on IVDs undergoing IVDD. This study was aiming to evaluate the effects of WBV intervention on the development and progression of IVDD mouse model induced by lumbar spine instability (LSI) surgery.

Methods

LSI surgery, by resecting the lumbar 3 rd -5 th spinous processes along with the supraspinous and interspinous ligaments, was conducted in 10-week-old male mice which then received WBV treatment (1 h per day, 5 days per week, at 3 Hz with peak acceleration at 0.4 g) or sham treatment. The progression of IVDD was evaluated by MRI, μCT and histological analyses after WBV treatment. The matrix metabolism, distribution of sensory nerves, pyroptosis in IVDs tissues were determined by immunohistological analysis or real-time PCR. The apoptosis of IVD cells was detected by TUNEL assay.

Results

LSI surgery was successful in producing IVDD modeling. WBV caused decreases in IVD height and annulus fibrosus (AF) score, as well as increased numbers of apoptotic cells in IVD tissues. WBV contributed to sensory innervation into AF and upregulation of Adamts5 and MMP3 expression in IVDD mice received LSI surgery. In addition, WBV treatment triggered earlier activation of Wnt/β-catenin signaling in IVDD mice with WBV treatment compared with those without WBV treatment. Unexpectedly, WBV significantly attenuated Caspase-1 and IL-1β expression in AF.

Conclusions

Collectively, our findings demonstrate that WBV treatment may worsen the development of ongoing IVDD. Decrease of IL-1β expression after WBV intervention may partially account for patient self-reported pain relief after WBV treatment in some previous trials. This study may help us better understand the effects of WBV intervention on patients experiencing LBP resulting from the degeneration of lumbar IVDs.

Background

Low back pain (LBP) is a major cause of disability, affecting approximately 0.6 billion individuals world-widely [1]. LBP is associated with high costs of health care and has abundant economic consequences due to loss of productivity from back pain-associated disability. Despite extensive studies that have

confirmed the intervertebral disc (IVD) degeneration (IVDD) is clinically associated with LBP and acknowledged as the main cause for LBP, the exact mechanism of discogenic back pain has not been elucidated [2, 3]. Currently, the mechanisms, diagnostic strategy, and treatment of LBP and IVDD all remain controversial, and relapse is easy to occur after treatment [4, 5].

Whole-body vibration (WBV), the first and foremost applied for the treatment of osteoporosis [6], is currently been broadly adopted for a range of musculoskeletal disorders in clinical practice, including back pain [7], gait and balance [8], lower extremity strength training [9], knee osteoarthritis (OA) [10], and fracture healing [11]. Recently, growing attention has been focused on the efficacy and safety of WBV application for joint health and fitness industry, especially IVDD and LBP [7, 12]. Despite a considerable amount of trial researches have declared WBV could provide more or fewer benefits for patients with LBP [13, 14], whereas epidemiological studies reported WBV increased prevalence of LBP in workers exposed to vibration [15]. Furthermore, increasing the majority of basic studies believed that WBV may be detrimental to the morphology of joint itself [16, 17]. Nevertheless, investigation on the bone effects of different WBV frequencies demonstrated that WBV induces local effects in bone that differ based on the anatomic site (e.g., vertebrae, femur or tibia) [18]. And the majority of basic studies have focused on the effects of WBV on normal IVDs, rather than those suffering from back pain provoked by IVDD. Therefore, the widespread use of WBV still requires more efficacious and rigorous research-based evidence for addressing the effects of WBV on IVDs undergoing IVDD or LBP.

Previous studies have proved that Wnt/β-catenin signaling pathway is activated and involved in matrix degradation, apoptosis of IVD cells and following IVDD progression [19, 20]. In this study, we aimed to evaluate the roles of WBV intervention on the pathological and biochemical changes of an IVDD mouse model, C57BL/6J mice first received LSI surgery to induce IVDD model and further exposed to a commercial WBV platform for 8 weeks. The lumbar vertebrae were harvested to evaluate the effects of WBV on changes of water content, height, tissue morphology, matrix metabolism, distribution of sensory nerves of IVD, apoptosis and pyroptosis of IVD cells as well as the activity of the Wnt/β-catenin signaling. The results may raise our understanding regarding the effects of WBV on the degeneration of lumbar IVD of humans.

Materials And Methods

Chemicals and Reagents

Primary antibodies against Aggrecan (ab36861), Adamt5 (ab41037), Calcitonin gene-related peptide (Cgrp, ab81887) were purchased from Abcam (Cambridge, UK), Type II collagen (Col2,MAB1330) was purchased from Millipore (Billerica, MA, USA), IL-1β (bs-6319R) was purchased from Bioss (Woburn, MA, USA), Nod-like receptor protein-3 (Nlrp3, 19771-1-AP), Caspase-1 (22915-1-AP), and Lef1 (14972-1-AP) were purchased from Proteintech (Wuhan, China), Mmp3 (RLT4465) and β-catenin (RLM3403) were purchased from Ruiying Biological Co. (Jiangsu, China). Unless otherwise mentioned, all chemicals were purchased from Sigma-Aldrich (St. Louis, MO, USA).

Experimental Animals And Treatments

A total of 72 C57BL/6J male mice (8-week-old, 22 ± 2 g) were purchased from Shanghai Laboratory Animal Center and housed at Animal Care Facility of Chinese Medical University according to the institutional guidelines for laboratory animals. All the animal procedures were approved by the Ethical Committee of Zhejiang Chinese Medical University. All mice were randomly divided into LSI surgery group (IVDD group), WBV group and SHAM group (n = 24 per group).

After anesthetized with pentobarbital sodium, mice in the IVDD group and the WBV group were operated by resecting the lumbar 3rd – 5th (L3–L5) spinous processes along with the supraspinous and interspinous ligaments to induce instability of lumbar spine [21, 22] (Fig. 1a). Three days post-surgery, mice in the WBV group was further exposed to a commercial WBV platform (Jin Ri Li Co., Shenzhen, China) with a fixed frequency, amplitude, and duration of exposure (3 HZ with peak acceleration at 0.4 g, 1 h per day, 5 days per week) (Fig. 1b). Mice in the SHAM group were only treated with the detachment of the posterior paravertebral muscles from the L3–L5 vertebrae. L3–L5 vertebrae of mice were harvested at 0, 1, 2, 4 and 8 weeks after the LSI surgery for further analysis (n = 6 per group at the indicated time) (Fig. 1c).

MRI Evaluation

Mice underwent T_2-weighted lumbar MRI scan using a 3.0T MR scanning system (Philips, Holland) 8 weeks after LSI surgery. T_2-weighted sagittal sections were rendered using a fast spin-echo sequence with time to a repetition of 500 ms and a time to echo of 8 ms.

Micro Computed Tomography (μCT)

The lower thoracic and whole lumbar spine from mice were dissected, fixed in 4% buffered paraformaldehyde for 72 h, transferred into phosphate-buffered saline, and then examined by high-resolution μCT (Skyscan 1176; Bruker μCT, Kontich, Belgium). The ribs on the lower thoracic were included for the identification of L4-L5 IVD localization. Images were reconstructed and analyzed using NRecon v1.6 and CTAn v1.9 (Skyscan company, San Jose, CA, USA), respectively. Three-dimension model visualization software, CTVol v2.0 (Skyscan company, San Jose, CA, USA), was used to analyze parameters of the L4-L5 IVD with the half-height of the L4 and L5 vertebrae. The scanner was set at a voltage of 90 kV, a current of 300 μA, and a resolution of 9 μm per pixel to measure the IVD. A resolution 9 μm per pixel was set for the whole L5 vertebral body measurement. Coronal images of the L4-L5 IVD were used to perform three-dimension histo-morphometric analyses of IVD. IVD volume was defined by the region of interest to cover the whole invisible space between L_4 and L_5 vertebrae.

Histology, Immunohistochemistry (IHC), And Immunofluorescent (IF)

After fixed in 4% buffered Paraformaldehyde for 72 h, the tissues were decalcified in 14% EDTA (pH 7.4) for 21 days at room temperature, dehydrated and then embedded in paraffin. Five-micrometer-thick

coronal-oriented sections of the L4–L5 IVD, were processed for Safranin O/Fast green staining. A histological grading scale established by Norcross et al was developed and tested for the degree of IVDD in a blind fashion, with some modifications (Table 1) [23]. Immunostaining was performed using a standard protocol. Sections were incubated with primary antibodies to Aggrecan (1:300), Col2 (1:1000), Mmp3 (1:300), Adamt5 (1:300), Nlrp3 (1:800), Casepase1 (1:300), IL-1β (1:800), Cgrp (1:200), β-catenin (1:500) and Lef1 (1:300) at 4℃ overnight. For IHC staining, a horseradish peroxidase streptavidin detection system (ZSGB-BIO, Beijing, China) was subsequently used to detect the immunoactivity, followed by counterstaining with hematoxylin. For IF assay, the slides were incubated with secondary antibodies conjugated with fluorescence at room temperature for 1 h. DAPI staining was used to estimate the total cell number. The images were captured using a microscope (Olympus, Tokyo, Japan).

Table 1

Histological grading scale criteria based on Norcross et al.

Scores	Symptoms
Nucleus pulposus (NP)	
5 Large, bulging central cavity with abundant NP material; >2/3 (IVD) height; smooth borders with minimal disruption	
4 Slightly reduced central cavity size with some NP material present; >1/3 IVD height and < 2/3 IVD height; minimal border disruption may be present	
3 Markedly reduced and disrupted cavity with minimal NP material and compartmentalization; total cavity > 1/3 IVD height and < 2/3 IVD height	
2 Severe disruption of NP with minimal cavity; total cavity < 1/3 IVD height but > 0; consists only of a few small pockets lined by NP-like cells	
1 Complete obliteration of cavity with no NP-lined pockets	
Annulus fibrosus (AF)	
5 Discrete, well-opposed lamellae bulging outward with no infolding; minimal preparation defect with “simple radial clefting”	
4 Discrete lamellae, less well-opposed; minimal infolding may be present; fibers remain well-organized, but with “complex radial clefting”	
3 Moderate to severe infolding of discrete, relatively well-opposed lamellae; moderate fragmentation of lamellae; AF fibers remain well organized	
2 Severe infolding and distortion of poorly opposed lamellae; severe fragmentation of lamellae; small regions of disorganized fibrous material replacing central lamellae	
1 Severe infolding, distortion, and fragmentation of lamellae; extensive amount of disorganized fibrous material replacing central lamellae	
Cartilage endplate (EP)	
5 Neatly arranged chondrocytes without any lesion or ectopic bone formation	
4 Hyaline cartilage cells were replaced by the spindle-shaped chondrocytes, ectopic bone formation only located at the “junction”.	
3 Ectopic bone formation located at superior cartilage endplate with smooth cartilage surface	
2 Ectopic bone formation located at whole cartilage endplate with smooth cartilage surface	
1 Ectopic bone formation located at whole cartilage endplate with flawed cartilage surface	
This scale mainly scores the disruption of nucleus pulposus central cavity, cellularity and collagen fiber orientation of annulus fibrosus and the degree of ectopia ossification of cartilage endplate. Simple radial clefting = the presence of radial gaps between AF lamellae with minimal fragmentation; complex radial clefting = the presence of radial, transverse, and/or oblique gaps in the lamellae with significant fragmentation; junction = the triangle junction between the cartilage endplate and the annulus fibrosus.	

TUNEL Assay

The TUNEL assay for detecting DNA breaks in IVD tissues was performed with TUNEL BrightGreen Apoptosis Detection Kit according to the manufacturer's instruction (Vazyme Biotech, Nanjing, China). Negative controls were incubated in a TdT free-enzyme solution. The number of positive cells was quantified in three randomly selected fields of view using three sections from each sample. DAPI staining was used to estimate the total cell number.

Quantitative Real-time PCR

Total RNA was extracted from L4 - L5 IVD using TRIzol reagent (Invitrogen, CA, USA) following the manufacturer's protocol. The yield and purity of RNA were quantified using nanodrop 2000C spectrophotometer (Thermo, Massachusetts, USA) and 2 μg of RNA were reverse-transcribed into cDNA using the PrimeScript RT Reagent Kit protocol (Takara Bio, Dalian, China). Real-time PCR amplification was performed using murine gene-specific primers (Supplementary Table 1) and TB Green Premix Ex Taq II (Takara) to quantify the mRNA expression levels of Aggrecan, β-Catenin and Lef1. Target mRNA expression levels were normalized against β-actin. The relative expression levels were calculated using the $2^{-\Delta\Delta}$CT method [24].

Statistics Analysis

All the data were expressed as mean ± s.d., as indicated in figure legends. All data analyses were performed using SPSS 15.0 analysis software (SPSS Inc, Illinois, USA). Statistical differences between groups were determined using one-way analysis of variance (ANOVA) or Student's t-test. and the level of significance was defined as $P < 0.05$.

Results

WBV Treatment Aggravates the Progression of IVDD Induced by LSI Surgery

To determine the effect of WBV on the progression of IVDD, mice in the IVDD group and WBV group received an LSI surgery to induce IVDD model as previously described [25], and then mice in the WBV group received multiple repeated whole-body vibration for 8 weeks (Fig. 1b-c). MRI scan results showed that LSI surgery was successful in producing IVDD modeling, resulting in remarkable signal loss of T_2-weighted image in IVD of IVDD mice, whereas virtually no signal loss in that of the SHAM mice (Fig. 2a). Compared to the IVDD group, WBV treatment further aggravate the decline of signal intensity (Fig. 2b). The IVD height of mice generally increased from birth to 1-month old, and then remained stable before decreasing around 4-month old [25]. Since the reduction of IVD height is commonly regarded as a surrogate predictor of IVDD, we evaluated the disc height index (DHI) between the L4-L5 by μCT analysis. And we found DHI in IVD mice is gradually decreased and a significant difference of DHI was observed at 8-week post-surgery, compared with SHAM mice. Unfortunately, this notable decreased DHI was already exhibited in WBV mice 2-week post-surgery (Fig. 2c-d). Moreover, no other obvious difference in BS/TV,

Tb.N and Tb.Sp, was observed between the IVDD mice and WBV mice except for a notable decrease in Tb.Sp in WBV mice (Fig. 2d). And we speculate that the decrease of trabecular space may result from the increase of bone mass by WBV treatment as previously described [11, 26].

Histological analysis of L4–L5 IVD by Safranin O/Fast green staining subsequently showed that the SHAM mice had well-organized IVD structures, including large vacuoles with sufficient matrix content in NP, arranged regularly AF tissues without any tearing, and no ectopic bone formation in EP, whereas WBV aggravated the IVDD phenotype induced by LSI surgery, including more severity of fissures and folds in the interlamellar of AF tissues, reduction in height and vacuole sizes in NP, formation of ectopic bone in EP (Fig. 3a). The deterioration of IVDD was further assessed by the histological score. As shown in Fig. 3b, NP, AF and EP scores were decreased in LSI-treated mice and WBV-treated mice compared with SHAM-treated mice, and a significant decrease of AF score exhibited in IVDD-mice since 2-week post-surgery ($P < 0.05$), and appeared earlier in WBV mice since 1-week post-surgery (Fig. 3b). All these radiological and morphologic results proved that WBV has deleterious effects on LSI-induced IVDD mice.

WBV Stimulates Apoptosis Of IVD Cells Of IVDD Mice

Besides, apoptosis of IVD cells, a process of cellular suicide, has been found to participate in the degeneration of IVD [22, 27, 28]. We next investigated the effects of WBV on apoptosis of IVD cells by TUNEL assay. Consistent with previous results, LSI-surgery strongly induced apoptosis of IVD cells in IVDD mice, and this increase of apoptosis in IVD cells was further amplified after WBV intervention (Fig. 3c).

WBV Intensifies Matrix Degradation In IVDD Mice

We determined the effects of WBV on matrix degradation in IVD. As the most abundant type of proteoglycan and matrix in IVDs, the mRNA levels of Aggrecan was firstly quantified by qRT-PCR and the results demonstrated that LSI-surgery treatment significantly decreased Aggrecan mRNA levels of IVD since 1-week post-surgery, and no notable differences of Aggrecan mRNA levels between the LSI and WBV groups except a much lower expression in WBV mice were observed at 4-week post-surgery (Supplementary Fig. 1a). Then, IHC analysis of Aggrecan and Col-2 (Fig. 3a-b,e-f) showed markedly reduced expression of Aggrecan and Col-2 in IVDD mice. Similar expression patterns of Aggrecan and Col-2 were also observed in WBV mice, except a lower Aggrecan expression at 4-week post-surgery, compared with IVDD mice. Afterward, IHC results of Adamt5 and Mmp3, two matrix-degrading enzymes of IVD matrix, showed WBV further increased the high expression of Adamt5 and Mmp3 of IVD induced by LSI surgery at 4-week post-surgery and at 8-week post-surgery, respectively (Fig. 3c-f). These results suggested that WBV accelerates IVDD progression by increasing the matrix degradation of IVD tissue.

WBV Increases Innervation and Sensory Nerve Ingrowth into NP region of IVDD Mice

IVDD is thought to lead to LBP because of nerve ingrowth into the degenerate IVD [5]. Evidence from animal models and humans has revealed sensory innervation of lumbar IVD and sensory nerve ingrowth

into the inner layer of IVD, causing painful conditions [29–31]. To explore the distribution of constant nociceptive sensory nerves after WBV treatment, we further detected the expression of Cgrp, a specific marker of sensory nerves and a potent vasodilator that causes pain sensitization. IF results demonstrated IVDD mice exhibited a significant increase in the number of $Cgrp^+$ cells in AF and ectopic bone formation zone, and eventually Cgrp positive expression in the NP region. Surprisingly, WBV treatment further increases the number of $Cgrp^+$ cells in outer AF of IVDs. These results demonstrated that WBV promotes the innervation of IVD and sensory nerves ingrowth into the NP region of IVDD mice (Fig. 5a-b).

WBV Attenuates Caspase-1 And IL-1β Expression In IVDD Mice

Studies have found that a cause of discogenic LBP is IVD inflammation and axonal growth of afferent fibers innervating the disc, and IL-1β is a pain-related molecule that was significantly elevated in painful human IVD [32]. We have previously reported that Nlrp3 inflammasome-mediated pyroptosis is proinflammatory and produces an excessive level of cartilage-degrading cytokines, including IL-1β [33]. To date, the relationship between pyroptosis and IVDD is still obscure. We speculate pyroptosis may also participate in the progression of IVDD and WBV intervention. Thus, we examined the expression changes of IL-1β, Nlrp3 and Caspase-1 (two key proteins in pyroptosis). Unexpectedly, IHC results of Caspase-1 and IL-1β demonstrated that LSI-treated mice had significantly increased Caspase-1 and IL-1β levels in NP and AF, whereas WBV-treated mice exhibited decreased Caspase-1 and IL-1β in NP and AF ($P < 0.01$) (Fig. 6c-f). However, almost no difference in expression of Nlrp3 protein between IVDD mice and WBV mice was observed except a slight increase in Nlrp3 at 4-week post-surgery ($P < 0.05$) (Supplementary Fig. 1b, c). These findings indicated that WBV may have a pain relief effect on IVDD mice, partially due to the decrease of IL-1β and pyroptosis in IVD tissue.

WBV Activates Wnt/β-catenin Signaling Pathway Of IVDD Mice

The previous studies have demonstrated that β-catenin protein is up-regulated and activated in disc tissues from patients with disc degeneration [27]. We investigated whether the activity of Wnt/β-catenin signaling is involved in WBV intervention mediated aggravation of IVDD. As expected, IHC results of β-catenin gradually increased at 2-week and peaked at 4-week post-surgery in IVDD mice, compared with SHAM mice. However, a higher peak appeared at 1-week post-surgery (2.8 folds of that in IVDD mice) following WBV treatment, thereafter reduced to 48% of that in IVDD mice at 2-week post-surgery (Fig. 6a,b). We further determine the activity of Wnt/β-catenin signaling by analyzing the RNA expression levels of β-catenin and Lef1 (a target gene of Wnt/β-catenin signaling) in IVD tissues by qPCR analysis. Consistent with previous IHC results of β-catenin, β-catenin and Lef1 mRNA levels started to increase at 1-week and peaked at 2-week in IVDD mice, whereas WBV treatment advanced β-catenin and Lef1 mRNA levels to 1-week post-surgery, and gradually decreased later (Fig. 6c). These results suggest that LSI surgery leads to the activation of Wnt/β-catenin signaling, and WBV may accelerate and exacerbate the degeneration of IVDs through earlier and stronger activation of Wnt/β-catenin signaling.

Discussion

Given that WBV is being used clinically to treat musculoskeletal disorders, followup work should investigate the response of degenerative IVDs tissues to WBV, to better mimic and understand its clinical use in humans. Surprisingly, to our knowledge, little data has been attempted to determine the effect of WBV on morphological and biomechanical changes of animal models who already receiving IVDD model, whereas most previous studies have used healthy mice, and usually no degenerative changes have been found in IVDs [16, 17]. Moreover, there is an urgent need to raise understanding of the mechanisms why patients with LBP reported great pain relief after WBV treatment. In this study, we found WBV indeed aggravates IVDD progression, including greater signal loss in T_2-weighted image, advanced decrease in IVD height and AF scores (since 1-week after LSI surgery), larger numbers of apoptotic cells, acceleration of matrix catabolism, innervation into AF and ingrowth of sensory nerves into NP. In addition, WBV treatment results in earlier activation of Wnt/β-catenin signaling in IVDD mice.

Persistent inflammation in painful discs, and that the production of these molecules may be a major factor in discogenic LBP. Nlrp3-mediated pyroptosis is a new form of programmed inflammatory cell death that participates in the inflammatory response by releasing a plentiful of cartilage-degrading cytokines, including IL-1β [33]. After Nlrp3 binds its adaptor apoptosis-associated speck-like protein, pro-Caspase-1 will be recruited to assemble Nlrp3 inflammasome. After then, the active Caspase-1 was released from it and further to hydrolyzes pro-IL-1β into mature IL-1β [34]. Our previous finding was consistent with those of the latter study, which demonstrated Nlrp3 inflammasome-mediated pyroptosis was induced during the progression of OA [33, 34]. However, the role of pyroptosis during the progression of IVDD and WBV is not yet utterly understood. For the first time to our knowledge, we revealed that LSI-treatment significantly induces pyroptosis by increasing the protein levels of Nlrp3, Caspase-1 and IL-1β in IVDs. Interestingly, WBV treatment significantly reduced the LSI-induced upregulation of Caspase-1 and IL-1β. This finding suggests that increase of pyroptosis and IL-1β in IVDs may account for increasing LBP for human suffering with IVDD, and inhibition of pyroptosis and IL-1β in IVDs could be one crucial mechanism for WBV in the relieving the LBP, which is parallel with the results stated by trial researches that patient self-reported pain relieve after WBV treatment in human.

Pathological innervation of the disc by pain-sensing nerve fibers is thought to be a key component of discogenic pain [35, 36]. In this study, we found that IVDD mice exhibited a significant increase in the number of $Cgrp^+$ sensory nerves both in outer AF and ectopic bone formation zone, and WBV treatment further increases the density of $Cgrp^+$ sensory nerves in outer AF. These results further indicate that more nociceptive sensory innervation in AF could be an important origin of LBP in IVDD patients. Yet, the induction of nerve ingrowth into the disc was not explicitly investigated. Previous studies have reported not all degenerative discs are symptomatic, and vice-versa [37]. Base on our current results, we hypothesize that any general consideration of LBP should pay close attention to the discs, not only water content, disc height, viscoelastic behavior, strength of the vertebrae as indicated by water content (MRI), or bone density (CT) and even levels of the local cytokines (IL-1β) in IVDs, but also the number and localization of sensory nerves in IVDs. Despite trial researches have reported WBV could alleviate pain in human LBP caused by various spinal-related diseases [13, 14], short duration of WBV treatment on LBP

showed that the effects of WBV alleviating LBP seem to be temporary, when the vibration ceased, LBP returned to pre-vibration levels [38]. For these reasons, we speculate that pain relief requires long-term use of WBV to be sustainable and effective, the source of LBP cannot be eliminated fundamentally. Also, for LBP patients who have already started to use WBV, if they stop using WBV for a period of time, their LBP may be aggravated due to the innervation into IVDs induced by WBV intervention.

Interestingly, parallel with numerous work, our recent finding demonstrated that WBV could be beneficial to fracture healing in ovariectomized rats with bone fracture model, which indicated that WBV may be favorable to fractures healing in individuals with postmenopausal osteoporosis [26]. Of concern is the fact that the effects of WBV on joint tissues have not been thoroughly evaluated. There is a serious polarization in the understanding of WBV's effects on joint health [13–17]. It should be noted that there is currently no consensus on the relative importance of specific parameters of WBV (e.g., amplitude, frequency and duration of exposure) on bone adaptation, because recent trial reports showed contradictory results [39]. Based on previous studies that demonstrated beneficial effects of WBV on muscle and bone [12]. The parameters of WBV (3 Hz, and 0.4 g peak acceleration) used in the current study were selected to introduce the specific value of peak acceleration and frequency, which are comparable to those equipment used for human joint health and considered safe by ISO-2631 [12], and parameters of WBV also fall within the average range of vibrations produced in common environments [37]. Therefore, one limitation of this study is that the IVDD mice are only intervened with WBV of fixed frequency and amplitude for IVDD mice. Thus, our findings may be incomprehensive to evaluate the potential benefits for IVDs if exposed to even greater acceleration during WBV intervention. Further studies on the effects of WBV with a range of amplitudes and high frequencies corresponding to those used in the usual WBV vehicles on an ongoing IVDD model will give us more comprehensive insights.

Previous studies have proved that the Wnt/β-catenin signaling pathway is activated in a degenerative joint disease like OA [40–43]. In vitro studies have reported activation of Wnt/β-catenin signaling leads to induction of cell cycle arrest and apoptosis of IVD cells, increases of matrix catabolic degradation enzymes to accelerate matrix degradation, thereby promoting IVD degeneration [19, 44, 45]. However, the relationship between WBV and Wnt/β-catenin signaling in IVDD mice is largely elusive. Our results found that WBV not only contributes to earlier and stronger activation of Wnt/β-catenin signaling in IVDD mice but also augments LSI surgery-induced apoptosis of IVD cells and expression levels of Adamts5 and Mmp3 proteins. Furthermore, a previous study on osteoporosis treatment has reported that suppressing Wnt/β-catenin pathway could upregulate the expression level of Nlrp3 and active-IL-1β in osteoblasts,which means Wnt/β-catenin pathway negatively regulates the activation of pyroptosis. Whether activation of Wnt/β-catenin signaling is associated with the pyroptosis inhibition in IVD and sensory innervation into AF is still obscure. Further researches need to be undertaken to determine their relationships in IVDD and WBV intervention.

We think another significance of our findings lies in the fact that although disc degeneration and LBP are often connected with each other, sometimes they are separated. Prior clinical studies have demonstrated that the presence of IVDD pathology is also present in a large proportion of asymptomatic individuals. On

the contrary, some patients have severe LBP with the absence of pathological changes of IVDD[46–48]. And there are no corresponding reports and suitable models for animal experiments. Characteristics of WBV mice could provide the possibility to further exploration of this clinical phenomenon.

Conclusions

To sum up, our foundings demonstrate that WBV treatment promotes matrix degradation, apoptosis of IVD cells and innervation of sensory nerves into IVD tissue to finally aggravate the development of ongoing IVDD via activation of Wnt/β-catenin signaling. In addition, WBV intervention decreases pyrotosis mediated IL-1β expression in IVD cells induced by LSI surgery may partially account for patients' self-reported pain relief after WBV treatment in previous trial researches. And it may help us better understand the effects of WBV intervention on humans experiencing LBP results from the degeneration of lumbar IVDs.

Abbreviations

WBV: Whole body vibration; LBP: low back pain; IVD: Intervertebral disc; IVDD: Intervertebral disc degeneration; LSI: Lumbar spine instability; EP: Endplate; AF: Annulus fibrosus; NP: nucleus pulposus; OA: osteoarthritis; Cgrp: Calcitonin gene-related peptide; Col2: Type II collagen; Nlrp3: Nod-like receptor protein-3; MRI: magnetic resonance imaging; μCT: Micro Computed Tomography; IHC: Immunohistochemistry; IF: Immunofluorescent; DHI: disc height index.

Declarations

Acknowledgements

This work was supported by the medical imaging department, the First Affiliated Hospital of Zhejiang Chinese Medical.

Authors' contributions

F.F., D.C. and H.R. prepared the article, H.R., C.W., D.C., P.T. and H.J. design the study and corrected the manuscript; F.F., S.Y., Z.S. and C.Z. performed the main investigation, Y.H. and H.L. scanned the micro-CT samples; F.F and Z.P. scanned the MRI samples; L.H. performed the statistical analysis and all authors agree to submit the article for publication. All funding sources had no involvement in the aforementioned process.

Funding

This study was supported by the Natural Science Foundation of Zhejiang Province (No.: LY19H270006, LQ17H270005), the National Natural Science Foundation of China (No.: 81973870, 81804121, 81573994), China Postdoctoral Science Foundation (No.: 2018M632154), the Traditional Chinese

Medical Administration of Zhejiang Province (No.: 2017ZB026), Zhejiang medical and health science and technology project (2018269058), Zhejiang Chinese medical university scientific research fund project (No.: 2018ZG20), the Science and technology innovation program for college students (new talent program) of Zhejiang Province (No.: 2018R410030), Opening Project of Zhejiang Provincial Preponderant and Characteristic Subject of Key University (Chinese Traditional Medicine), Zhejiang Chinese Medical University (No.: ZYX2018008), Plan Guide Project of HangZhou Technology Department (No.: 20171226Y98), Plan technology project of HangZhou Health Department (No.: 2018B028).

Ethics approval and consent to participate

The animal studies were approved by the Ethical Committee of Zhejiang Chinese Medical University.

Consent for publication

All authors approved the final version of the manuscript to be published.

Competing interests

The authors declare that they have no competing interests.

Author details

[a]Institute of Orthopaedics and Traumatology, the First Affiliated Hospital of Zhejiang Chinese Medical University, Hangzhou 310053, Zhejiang Province, China

[b]Department of Pharmacy, the Second Affiliated Hospital, Zhejiang University School of Medicine, Hangzhou 310009, China

[c]Department of Orthopedics, Shenzhen Traditional Chinese Hospital, Guangzhou University of Chinese Medicine, Shenzhen 518055, China

[d]Research Center for Human Tissues and Organs Degeneration, Shenzhen Institutes of Advanced Technology, Chinese Academy of Sciences, Shenzhen 518055, China

[e]Longhua Hospital Affiliated to Shanghai University of Traditional Chinese Medicine，Shanghai 200032, China

[f]First Clinical College of Zhejiang Chinese Medical University, Hangzhou 310053, Zhejiang, China

References

1. Vos T, Flaxman AD, Naghavi M, Lozano R, Michaud C, Ezzati M, et al. Years lived with disability (YLDs) for 1160 sequelae of 289 diseases and injuries 1990-2010: a systematic analysis for the Global Burden of Disease Study 2010. Lancet. 2012;380:2163-96.

2. Hoy D, Bain C, Williams G, March L, Brooks P, Blyth F, et al. A systematic review of the global prevalence of low back pain. Arthritis Rheum. 2012;64:2028-37.
3. Sakai D, Grad S. Advancing the cellular and molecular therapy for intervertebral disc disease. Adv Drug Deliv Rev. 2015;84:159-71.
4. Virtanen IM, Karppinen J, Taimela S, Ott J, Barral S, Kaikkonen K, et al. Occupational and genetic risk factors associated with intervertebral disc disease. Spine (Phila Pa 1976). 2007;32:1129-34.
5. Loibl M, Wuertz-Kozak K, Vadala G, Lang S, Fairbank J, Urban JP. Controversies in regenerative medicine: Should intervertebral disc degeneration be treated with mesenchymal stem cells. JOR Spine. 2019;2:e1043.
6. Rubin C, Recker R, Cullen D, Ryaby J, McCabe J, McLeod K. Prevention of postmenopausal bone loss by a low-magnitude, high-frequency mechanical stimuli: a clinical trial assessing compliance, efficacy, and safety. J Bone Miner Res. 2004;19:343-51.
7. Perraton L, Machotka Z, Kumar S. Whole-body vibration to treat low back pain: fact or fad. Physiother Can. 2011;63:88-93.
8. Bruyere O, Wuidart MA, Di Palma E, Gourlay M, Ethgen O, Richy F, et al. Controlled whole body vibration to decrease fall risk and improve health-related quality of life of nursing home residents. Arch Phys Med Rehabil. 2005;86:303-7.
9. Bogaerts A, Delecluse C, Claessens AL, Coudyzer W, Boonen S, Verschueren SM. Impact of whole-body vibration training versus fitness training on muscle strength and muscle mass in older men: a 1-year randomized controlled trial. J Gerontol A Biol Sci Med Sci. 2007;62:630-5.
10. Park YG, Kwon BS, Park JW, Cha DY, Nam KY, Sim KB, et al. Therapeutic effect of whole body vibration on chronic knee osteoarthritis. Ann Rehabil Med. 2013;37:505-15.
11. Wehrle E, Wehner T, Heilmann A, Bindl R, Claes L, Jakob F, et al. Distinct frequency dependent effects of whole-body vibration on non-fractured bone and fracture healing in mice. J Orthop Res. 2014;32:1006-13.
12. Muir J, Kiel DP, Rubin CT. Safety and severity of accelerations delivered from whole body vibration exercise devices to standing adults. J Sci Med Sport. 2013;16:526-31.
13. Belavý DL, Hides JA, Wilson SJ, Stanton W, Dimeo FC, Rittweger J, et al. Resistive simulated weightbearing exercise with whole body vibration reduces lumbar spine deconditioning in bed-rest. Spine (Phila Pa 1976). 2008;33:E121-31.
14. Wang XQ, Gu W, Chen BL, Wang X, Hu HY, Zheng YL, et al. Effects of whole-body vibration exercise for non-specific chronic low back pain: an assessor-blind, randomized controlled trial. Clin Rehabil. 2019;33:1445-57.
15. Bovenzi M. Low back pain disorders and exposure to whole-body vibration in the workplace. Semin Perinatol. 1996;20:38-53.
16. McCann MR, Patel P, Pest MA, Ratneswaran A, Lalli G, Beaucage KL, et al. Repeated exposure to high-frequency low-amplitude vibration induces degeneration of murine intervertebral discs and knee joints. Arthritis Rheumatol. 2015;67:2164-75.

17. Kerr GJ, McCann MR, Branch JK, Ratneswaran A, Pest MA, Holdsworth DW, et al. C57BL/6 mice are resistant to joint degeneration induced by whole-body vibration. Osteoarthritis Cartilage. 2017;25:421-5.
18. Pasqualini M, Lavet C, Elbadaoui M, Vanden-Bossche A, Laroche N, Gnyubkin V, et al. Skeletal site-specific effects of whole body vibration in mature rats: from deleterious to beneficial frequency-dependent effects. Bone. 2013;55:69-77.
19. Hiyama A, Sakai D, Risbud MV, Tanaka M, Arai F, Abe K, et al. Enhancement of intervertebral disc cell senescence by WNT/β-catenin signaling-induced matrix metalloproteinase expression. Arthritis Rheum. 2010;62:3036-47.
20. Ye S, Wang J, Yang S, Xu W, Xie M, Han K, et al. Specific inhibitory protein Dkk-1 blocking Wnt/β-catenin signaling pathway improve protectives effect on the extracellular matrix. J Huazhong Univ Sci Technolog Med Sci. 2011;31:657.
21. Miyamoto S YK, Ono K. Experimental cervical spondylosis in the mouse. Spine (Phila Pa 1976). 1991;16 (10 Suppl):S495–S500.
22. Ariga K MS, al NTe. The relationship between apoptosis of endplate chondrocytes and aging and degeneration of the intervertebral disc. Spine (Phila Pa 1976). 2001;26:2414–2420.
23. Norcross JP LGE, Weinhold P DLE. An in vivo model of degenerative disc disease. J Orthop Res. 2003;21:183-8.
24. Livak KJ, Schmittgen TD. Analysis of relative gene expression data using real-time quantitative PCR and the 2(-Delta Delta C(T)) Method. Methods. 2001;25:402-8.
25. Qin Bian LM, Amit Jain JLC, Khaled Kebaish MW, Zhengdong Zhang XEG, Paul D Sponseller CAS, Lee H Riley YWaXC. Mechanosignaling activation of TGFβ maintains intervertebral disc homeostasis. Bone Res. 2017;5:17008.
26. Chen J, Ruan H, Liu Y, Bao J, Xu H, Yao M, et al. Therapeutic effects of whole-body vibration on fracture healing in ovariectomized rats: a systematic review and meta-analysis. Menopause. 2018;26:677-86.
27. Sun Z, Jian Y, Fu H, Li B. MiR-532 downregulation of the Wnt/β-catenin signaling via targeting Bcl-9 and induced human intervertebral disc nucleus pulposus cells apoptosis. J Pharmacol Sci. 2018;138:263-70.
28. Zhang HJ, Ma XH, Xie SL, Qin SL, Liu CZ, Zhang ZG. Knockdown of miR-660 protects nucleus pulposus cells from TNF-a-induced apoptosis by targeting serum amyloid A1. J Orthop Surg Res. 2020;15:7.
29. Takahashi Y, Nakajima Y, Sakamoto T, Moriya H, Takahashi K. Capsaicin applied to rat lumbar intervertebral disc causes extravasation in the groin skin: a possible mechanism of referred pain of the intervertebral disc. Neurosci Lett. 1993;161:1-3.
30. Chen J, Hou S, Peng B, Wu W, Shi Y, Li L, et al. Effect of the L2 ramus communicans on the nociceptive pathway in lumbar intervertebral discs in rats. Eur J Pain. 2008;12:798-803.

31. Ohtori S, Miyagi M, Inoue G. Sensory nerve ingrowth, cytokines, and instability of discogenic low back pain: A review. Spine Surg Relat Res. 2018;2:11-7.
32. Kepler CK, Markova DZ, Dibra F, Yadla S, Vaccaro AR, Risbud MV, et al. Expression and relationship of proinflammatory chemokine RANTES/CCL5 and cytokine IL-1β in painful human intervertebral discs. Spine (Phila Pa 1976). 2013;38:873-80.
33. Hu J, Zhou J, Wu J, Chen Q, Du W, Fu F, et al. Loganin ameliorates cartilage degeneration and osteoarthritis development in an osteoarthritis mouse model through inhibition of NF-κB activity and pyroptosis in chondrocytes. J Ethnopharmacol. 2020;247:112261.
34. Haseeb A, Haqqi TM. Immunopathogenesis of osteoarthritis. Clin Immunol. 2013;146:185-96.
35. Leimer EM, Gayoso MG, Jing L, Tang SY, Gupta MC, Setton LA. Behavioral Compensations and Neuronal Remodeling in a Rodent Model of Chronic Intervertebral Disc Degeneration. Sci Rep. 2019;9:3759.
36. Romereim SM, Johnston CA, Redwine AL, Wachs RA. Development of an in vitro intervertebral disc innervation model to screen neuroinhibitory biomaterials. J Orthop Res. 2019.
37. Hill TE, Desmoulin GT, Hunter CJ. Is vibration truly an injurious stimulus in the human spine. J Biomech. 2009;42:2631-5.
38. Lurie RC, Cimino SR, Gregory DE, Brown S. The effect of short duration low back vibration on pain developed during prolonged standing. Appl Ergon. 2018;67:246-51.
39. Torcasio A, van Lenthe GH, Van Oosterwyck H. The importance of loading frequency, rate and vibration for enhancing bone adaptation and implant osseointegration. Eur Cell Mater. 2008;16:56-68.
40. De Santis M, Di Matteo B, Chisari E, Cincinelli G, Angele P, Lattermann C, et al. The Role of Wnt Pathway in the Pathogenesis of OA and Its Potential Therapeutic Implications in the Field of Regenerative Medicine. Biomed Res Int. 2018;2018:7402947.
41. Okura T, Ohkawara B, Takegami Y, Ito M, Masuda A, Seki T, et al. Mianserin suppresses R-spondin 2-induced activation of Wnt/β-catenin signaling in chondrocytes and prevents cartilage degradation in a rat model of osteoarthritis. Sci Rep. 2019;9:2808.
42. Wang X, Cornelis F, Lories RJ, Monteagudo S. Exostosin-1 enhances canonical Wnt signaling activity during chondrogenic differentiation. Osteoarthritis Cartilage. 2019.
43. Xie WQ, Zhao YJ, Li F, Shu B, Lin SR, Sun L, et al. Velvet antler polypeptide partially rescue facet joint osteoarthritis-like phenotype in adult β-catenin conditional activation mice. BMC Complement Altern Med. 2019;19:191.
44. Wang X, Zou M, Li J, Wang B, Zhang Q, Liu F, et al. LncRNA H19 targets miR-22 to modulate H2 O2 -induced deregulation in nucleus pulposus cell senescence, proliferation, and ECM synthesis through Wnt signaling. J Cell Biochem. 2018;119:4990-5002.
45. Zhan S, Wang K, Song Y, Li S, Yin H, Luo R, et al. Long non-coding RNA HOTAIR modulates intervertebral disc degenerative changes via Wnt/β-catenin pathway. Arthritis Res Ther. 2019;21:201.

46. Steffens D, Hancock MJ, Maher CG, Williams C, Jensen TS, Latimer J. Does magnetic resonance imaging predict future low back pain? A systematic review. Eur J Pain. 2014;18:755-65.
47. Kalichman L, Kim DH, Li L, Guermazi A, Hunter DJ. Computed tomography-evaluated features of spinal degeneration: prevalence, intercorrelation, and association with self-reported low back pain. Spine J. 2010;10:200-8.
48. Brinjikji W, Diehn FE, Jarvik JG, Carr CM, Kallmes DF, Murad MH, et al. MRI Findings of Disc Degeneration are More Prevalent in Adults with Low Back Pain than in Asymptomatic Controls: A Systematic Review and Meta-Analysis. AJNR Am J Neuroradiol. 2015;36:2394-9.

Figures

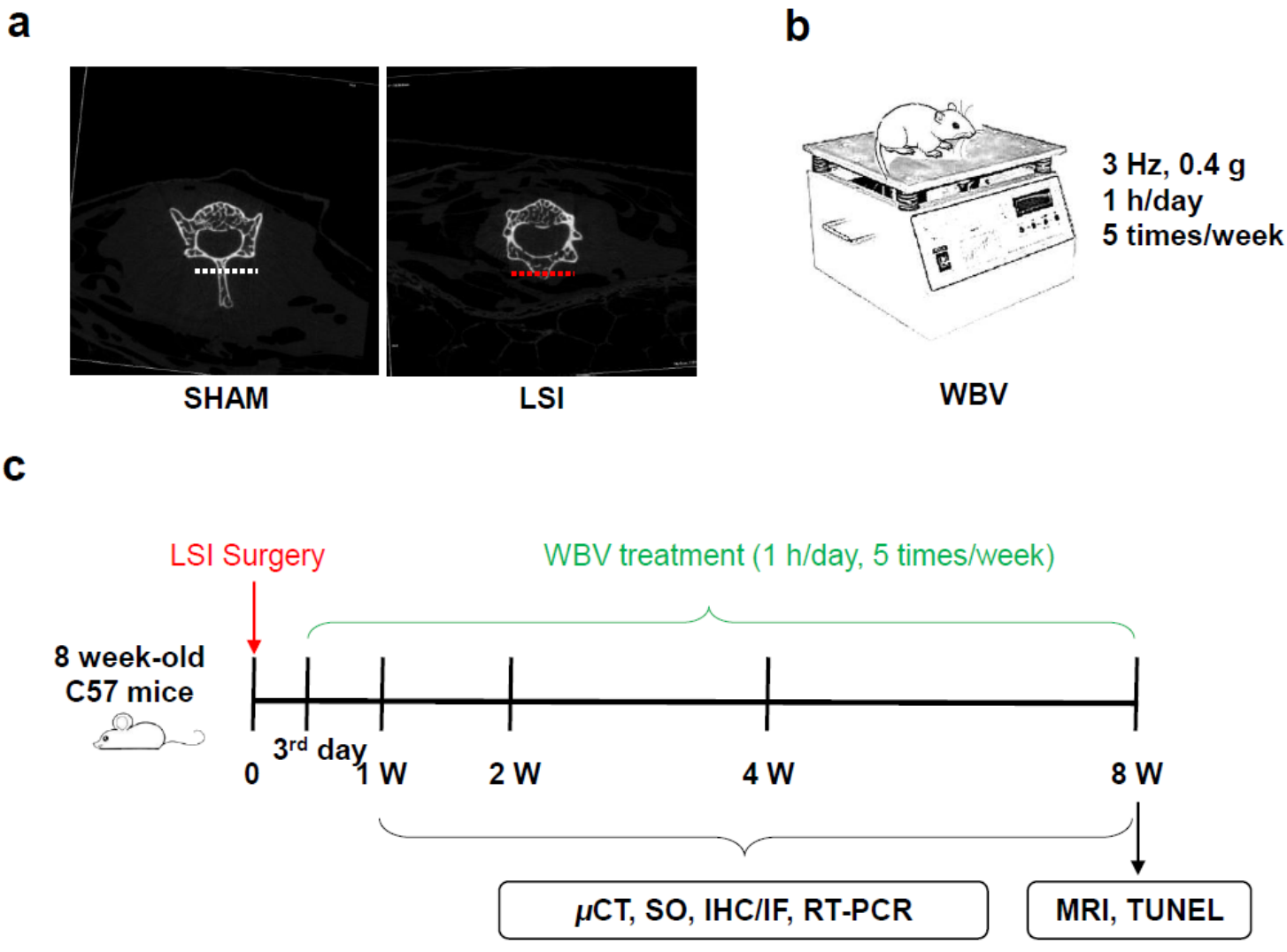

Figure 1

Animal treatment and study design of the project. a Lumbar spine instability (LSI)-induced IVDD mouse model. Mouse L3–L5 spinous processes were resected along with the supraspinous and interspinous ligaments (red dotted line in LSI group) to induce instability of lumbar spine. b Whole-body vibration

(WBV) treatment. Three days after the LSI surgery, mice in the WBV group were further received with WBV in a commercially available horizontal vibration device (3 Hz, 0.4 g, 1 h/day, 5 times per week). c Study design of the project.

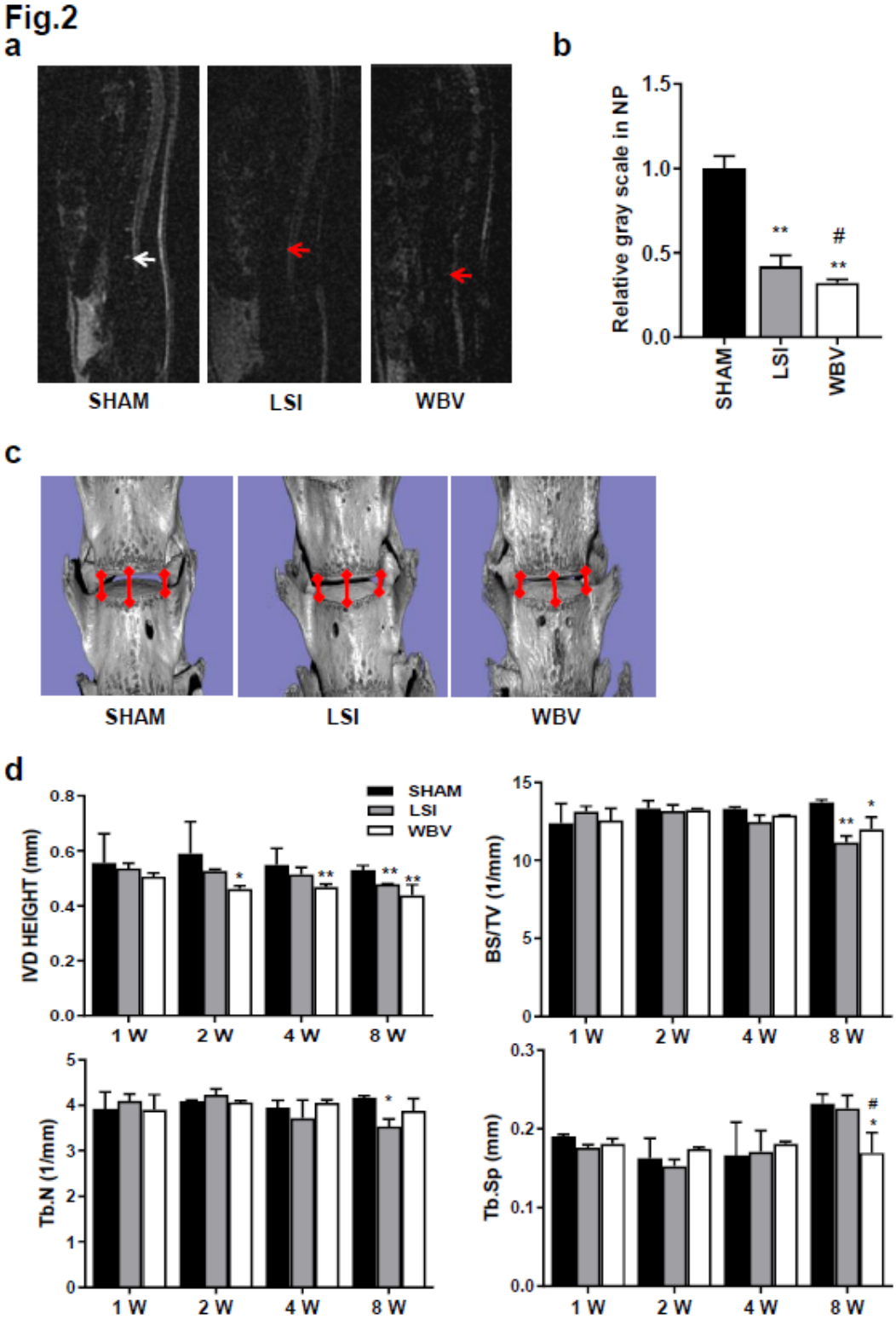

Figure 2

WBV treatment further aggravates the decline of signal intensity and IVD height of IVDD mice model induced by LSI surgery. a T2-weighted magnetic resonance imaging (MRI) of intervertebral discs. White

arrow indicated healthy discs in the SHAM group own brighter signal on MRI due to the presence of an expected amount of water. Red arrow in the LSI group and WBV group indicate a more significant decrease in disc signal, causing the discs to appear darker on MRI. b Quantification of grayscale of L4-L5 disc on a. c Micro-computed tomography (μCT) of the lumbar spine. The red double-headed arrows represent the distance between the middle to middle or side to side of the adjacent vertebra. d Intervertebral L4–L5 disc height and bone histomorphometry (BS/TV, Tb.N, Tb.Sp) of L5 vertebral body were analyzed at 1-, 2-, 4-, and 8-week (W) post-surgery. Data are shown as mean ± s.d. *P < 0.05, **P < 0.01 compared with SHAM group; #P < 0.05, ##P < 0.01 compared with IVDD group.

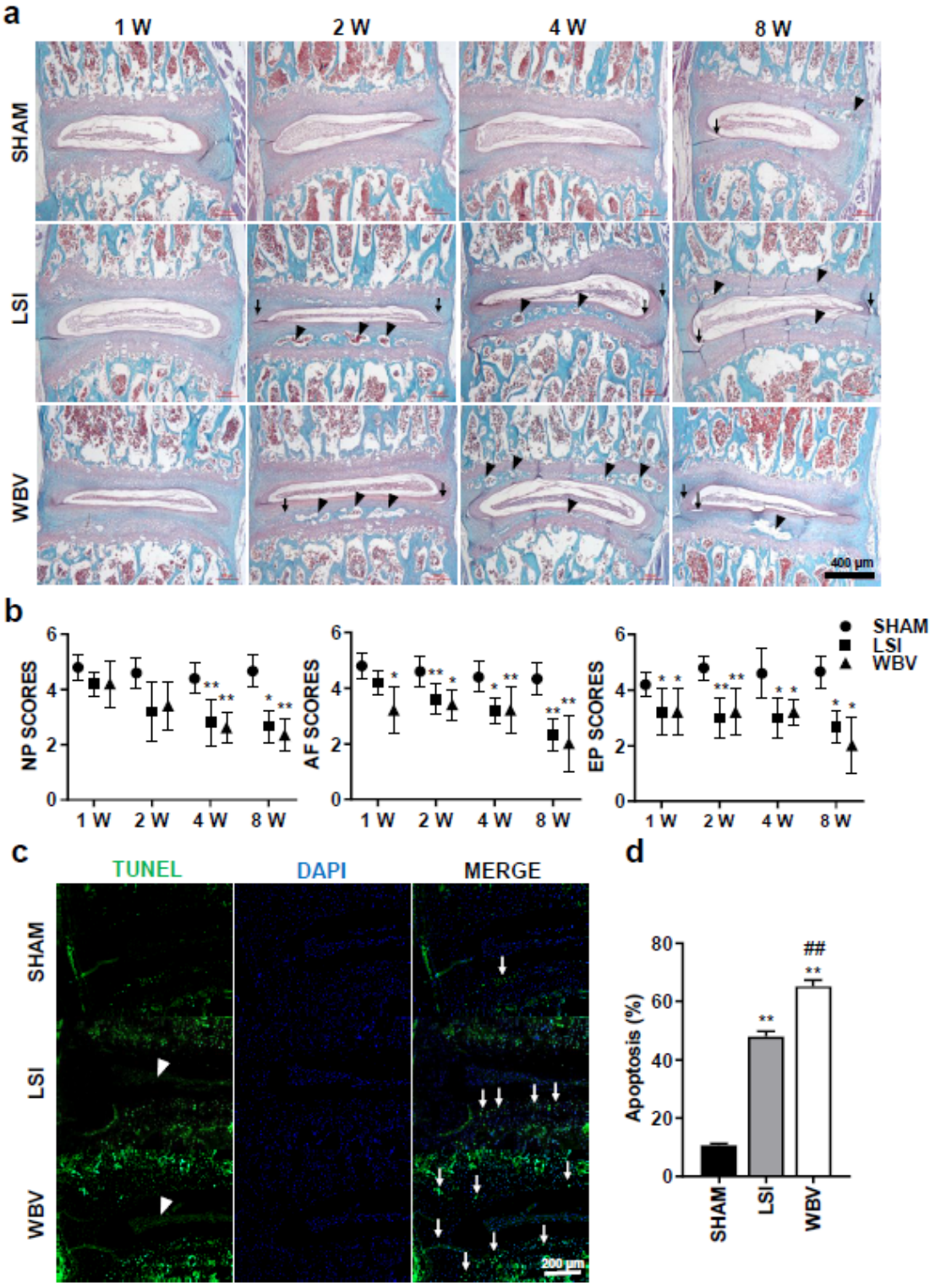

Figure 3

WBV treatment further deteriorates morphologic changes of IVD tissue and apoptosis of IVD cells of IVDD mice. a Representative Safranin O staining images of the IVD sections showing the changes of IVD cells in SHAM, IVDD and WBV mice at 1-, 2-, 4- and 8-week post-surgery. b Evaluation of IVD degeneration by NP, AF and EP score. c Apoptosis images of the IVD sections. DAPI stains nuclei blue. Whiteheads indicate apoptosis in NP cells, White arrows indicate apoptosis in EP cells. d Quantification of apoptosis

rate in c. Data are shown as mean ± s.d. Three independent experiments performed in triplicate. *P < 0.05, **P < 0.01 compared with SHAM group, #P < 0.05, ##P < 0.01 compared with IVDD group.

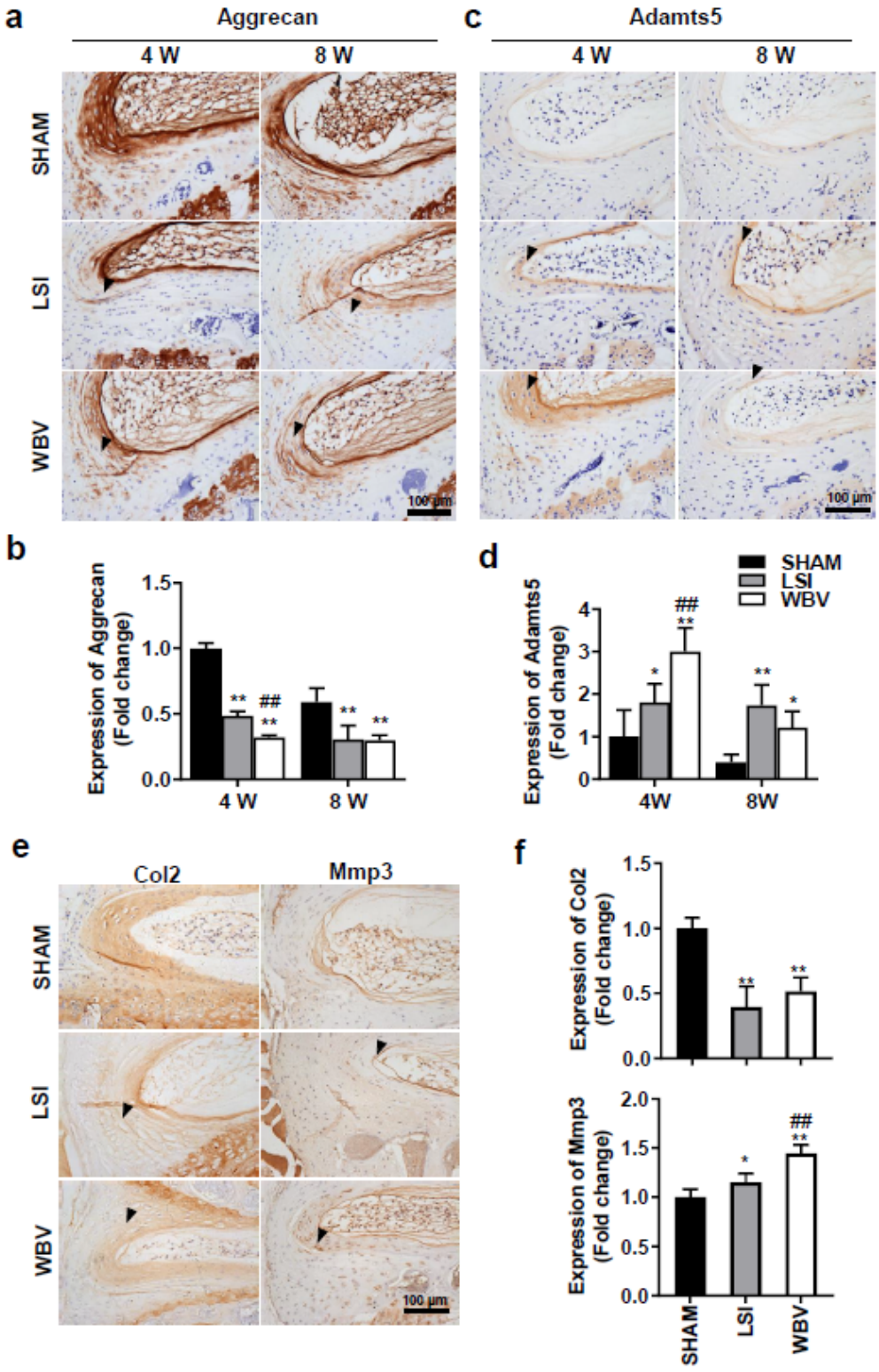

Figure 4

WBV treatment resultes in matrix composition changes in the IVDs of IVDD mice. a Immunostaining for Aggrecan in the IVD (brown) at 4-, 8- week (W) post-surgery. Hematoxylin stains nuclei purple. Black arrowheads indicate a low expression of Aggrecan in AF. b Quantification of Aggrecan expression in a. c

Immunostaining for Adamts5 in the AF (brown) at 4-, 8-week post-surgery. Black arrowheads indicate high expression of Aggrecan in AF. d Quantification of Adamts5 expression in c. e Immunostaining for Col2 and MMP3 (brown) at 8-week post-surgery. Black arrowheads indicate low expression of Col2 in AF or high expression of Mmp3 in AF. f Quantification of Col2 and Mmp3 expression in e. Data are shown as mean ± s.d. Three independent experiments were performed in triplicate. *P < 0.05, **P < 0.01 compared with SHAM group, #P < 0.05, ##P < 0.01 compared with IVDD group.

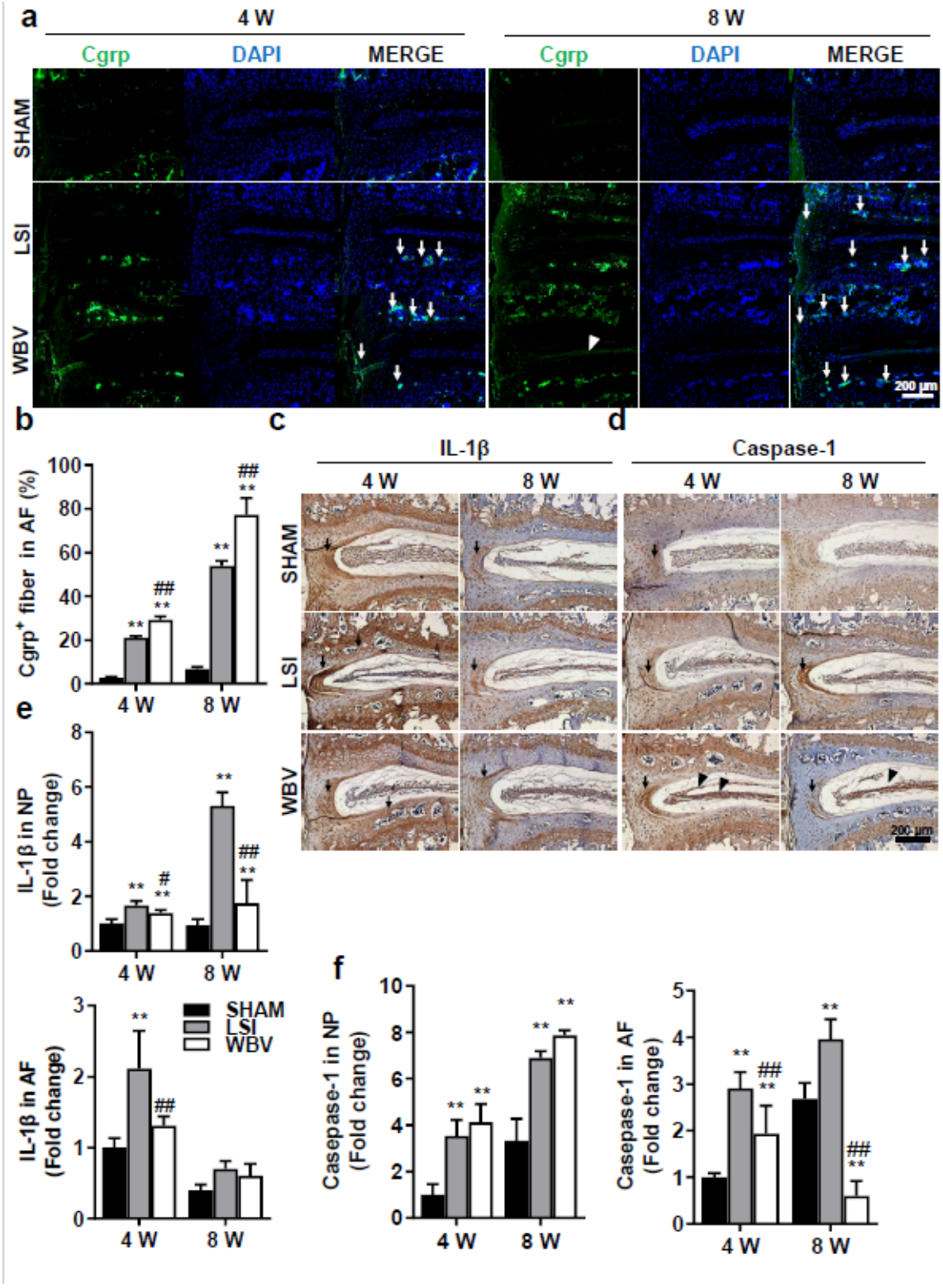

Figure 5

WBV treatment further stimulates innervation and ingrowth of sensory nerves but reduces LSI surgery-induced upregulation of pyroptosis in IVDs of IVDD mice. a Immunofluorescence staining for Cgrp expression (green) at 4- and 8-week (W) post-surgery. DAPI stains nuclei blue. White arrows indicate high expression of Cgrp in the ectopic bone formation zone of EP and outer AF; White arrowheads indicate high expression of Cgrp in NP. b Quantification of Nlrp3+ cells in a. c, d Immunostaining for IL-1β c and Caspase-1 d in the IVD (brown) at 4- and 8-week post-surgery. Hematoxylin stains nuclei purple. Black arrowheads indicate high expressions of Caspase-1 in NP. Black arrows indicate high expressions of Caspase-1 and IL-1β in AF. e, f Quantification of and IL-1β and Caspase-1 expression in c and d. Data are shown as mean ± s.d. Three independent experiments were performed in triplicate. Data are shown as mean ± s.d. Three independent experiments were performed in triplicate. *P < 0.05, **P < 0.01 compared with SHAM group; #P < 0.05, ##P < 0.01 compared with IVDD group.

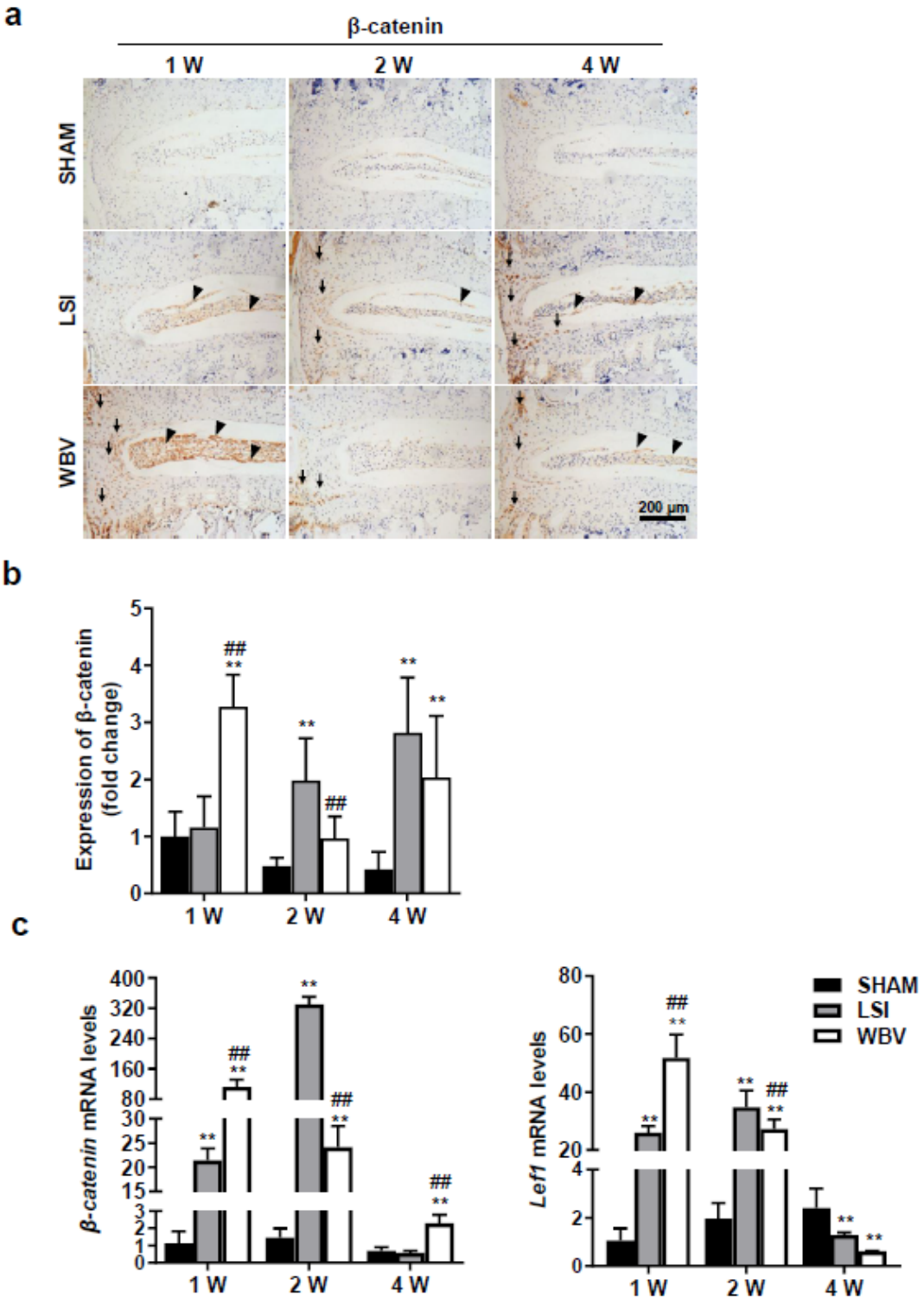

Figure 6

WBV treatment further activates Wnt/β-catenin signaling pathway in IVDs of IVDD mice. a Immunostaining for β-catenin in the IVD tissues at 1-, 2- and 4-week (W) post-surgery (brown). Hematoxylin stains nuclei purple. Black arrowheads indicate high expression of β-catenin in NP. Black arrows indicate high expression of β-catenin in AF. b Quantification of β-catenin expression in a. c qPCR analysis for β-catenin, Lef1 in the IVD at 1-, 2- and 4-week (W) post-surgery. Data are shown as mean ±

s.d. Three independent experiments were performed in triplicate. *P < 0.05, **P < 0.01 compared with SHAM group; #P < 0.05, ##P < 0.01 compared with IVDD group.

Supplementary Files

This is a list of supplementary files associated with this preprint. Click to download.

- Supplementaryfigures.pdf
- TableS1.docx